Phenology and species determine growing-season albedo increase at the altitudinal limit of shrub growth in the sub-Arctic

Article *in* Global Change Biology · May 2016

Impact Factor: 8.04 · DOI: 10.1111/gcb.13297

4 authors:

Scott N. Williamson

University of Alberta

13 PUBLICATIONS **73** CITATIONS

SEE PROFILE

Isabel C Barrio

University of Iceland

38 PUBLICATIONS **220** CITATIONS

SEE PROFILE

David S Hik

University of Alberta

137 PUBLICATIONS **4,276** CITATIONS

SEE PROFILE

John Gamon

University of Alberta

154 PUBLICATIONS **8,912** CITATIONS

SEE PROFILE

Global Change Biology

Global Change Biology (2016), doi: 10.1111/gcb.13297

Phenology and species determine growing-season albedo increase at the altitudinal limit of shrub growth in the sub-Arctic

SCOTT N. WILLIAMSON[1], ISABEL C. BARRIO[1,*], DAVID S. HIK[1] and JOHN A. GAMON[1,2]

[1]*Department of Biological Sciences, University of Alberta, Edmonton, AB T6G 2E9, Canada,* [2]*Department of Earth and Atmospheric Sciences, University of Alberta, Edmonton, AB T6G 2E3, Canada*

Abstract

Arctic warming is resulting in reduced snow cover and increased shrub growth, both of which have been associated with altered land surface–atmospheric feedback processes involving sensible heat flux, ground heat flux and biogeochemical cycling. Using field measurements, we show that two common Arctic shrub species (*Betula glandulosa* and *Salix pulchra*), which are largely responsible for shrub encroachment in tundra, differed markedly in albedo and that albedo of both species increased as growing season progressed when measured at their altitudinal limit. A moveable apparatus was used to repeatedly measure albedo at six precise spots during the summer of 2012, and resampled in 2013. Contrary to the generally accepted view of shrub-covered areas having low albedo in tundra, full-canopy prostrate *B. glandulosa* had almost the highest albedo of all surfaces measured during the peak of the growing season. The higher midsummer albedo is also evident in localized MODIS albedo aggregated from 2000 to 2013, which displays a similar increase in growing-season albedo. Using our field measurements, we show the ensemble summer increase in tundra albedo counteracts the generalized effect of earlier spring snow melt on surface energy balance by approximately 40%. This summer increase in albedo, when viewed in absolute values, is as large as the difference between the forest and tundra transition. These results indicate that near future (<50 years) changes in growing-season albedo related to Arctic vegetation change are unlikely to be particularly large and might constitute a negative feedback to climate warming in certain circumstances. Future efforts to calculate energy budgets and a sensible heating feedback in the Arctic will require more detailed information about the relative abundance of different ground cover types, particularly shrub species and their respective growth forms and phenology.

Keywords: albedo, alpine tundra, *Betula*, growing season, phenology, *Salix*

Received 15 October 2015; revised version received 2 March 2016 and accepted 18 March 2016

Introduction

Warming in the Arctic has been linked to spring and fall snow cover reduction which has extended snow-free periods in the south-west Yukon by ~11 days per decade in spring and ~2 days per decade in autumn between 1967 and 2008 (Zeng *et al.*, 2011; Brown *et al.*, 2010). Warming has also occurred with shrub expansion in many regions (Sturm *et al.*, 2001; Tape *et al.*, 2006, 2012; Frost & Epstein, 2014). Increased shrub growth and growing-season length have been predicted to increase sensible heating by reducing albedo (Chapin *et al.*, 2005), triggering a radiative feedback to climate that will promote further atmospheric warming (e.g. Pearson *et al.*, 2013). However, differences between shrub species, stature and phenology might also affect this albedo feedback and consequently alter simple predictions about future feedback processes (Oke, 1987), especially in a warmer (Snow, Water, Ice, Permafrost in the Arctic (SWIPA), 2011) and wetter (Cook *et al.*, 2014) Arctic. Similarly, warming in alpine tundra is also leading to increased shrub growth (Hallinger *et al.*, 2010), and it is generally accepted that shrub expansion will reduce albedo in both winter and summer (Sturm *et al.*, 2005). However, field measurements of tundra summer energy budgets and albedo are typically conducted over short periods (1–14 days; see review article by Eugster *et al.*, 2000) that often coincide with peak growing season, and lack sampling consistency between studies, especially when spatial averaging is applied. These sampling differences lead to uncertainty in albedo assessment, and the considerable range in the reported albedo values for most Arctic land cover (Eugster *et al.*, 2000) precludes accurate predictions of

*Present address: Institute of Life and Environmental Sciences, University of Iceland, Sturlugata 7, 101 Reykjavík, Iceland

Correspondence: Scott N. Williamson, tel. +1 780 492-4863, fax +1 780 492-9234, e-mail: snw@ualberta.ca

how changing feedback processes will affect tundra energy budgets.

Some temperate deciduous forests show an albedo increase as spring leaf out progresses from bare trees to full canopy (Moore *et al.*, 1996). Measurements of albedo in tundra for the whole of the growing season also show an increase in albedo after snow melt, suggesting growing-season vegetation albedo is more dynamic than fixed values allow. In snow-free, sparsely vegetated tundra, albedo increases with decreasing soil moisture as the growing season progresses (Harding & Lloyd, 1998). A study of mixed willow–birch in the sub-Arctic shows that albedo displays a growing season increase from 0.11 (prior to leaf emergence) to 0.16 after leaves have completely opened, which indicates that the canopy has progressively become more reflective of incoming shortwave radiation (Blanken & Rouse, 1994); however, individual species were not measured independently, leading to uncertainty in their contributions to albedo dynamics. The increase in albedo is strongly and positively correlated to leaf area index (LAI) for both deciduous trees and sedges (Lafleur *et al.*, 1987).

Shrub species identity, height and phenological changes in canopy structure affect albedo and should all be considered in detailed analyses of vegetation feedbacks to climate. Short deciduous shrubs (<0.5 m) of the genera *Betula* and *Salix* are largely responsible for shrub encroachment into tundra (Tape *et al.*, 2006; Euskirchen *et al.*, 2009). While both genera are predicted to increase in cover under warming scenarios, *Betula* spp. are likely to be more successful than *Salix* spp. in a warmer Arctic (Euskirchen *et al.*, 2009). Canopy structure also influences albedo with taller vegetation typically having lower albedo than shorter vegetation because taller vegetation is typically more effective at radiation trapping (Oke, 1987). Comparisons of species with contrasting heights confirmed that low shrubs have a consistently higher albedo than tall shrubs measured along a 50 m transect in Alaska early in the growing season, soon after snow melt (Sturm *et al.*, 2005). This decline in albedo with canopy height has also been observed along a 5 km transect extending from tundra, low shrub, tall shrub, woodland to forest (Thompson *et al.*, 2004). Phenological changes throughout the growing season may influence albedo values. For example, comparisons of albedo for both low and tall shrub categories following spring snow melt but prior to leaf emergence (Sturm *et al.*, 2005) with albedo measured at peak growing season (Thompson *et al.*, 2004) suggest an albedo increase of 0.03 – 0.04 during midsummer.

To better understand albedo dynamics associated with common Arctic land cover types, we measured albedo throughout the growing season at six sites identified *a priori* as being representative of the major alpine tundra land cover types in the south-west Yukon. Our precisely repeated measurements allowed us to account for differences associated with shrub species, canopy structure and height without the confounding effects of spatial averaging across multiple vegetation types. Our specific aim was to determine the growing-season albedo trends of tundra landscape cover characteristic of different stages of succession, measured near the upper elevational limit of shrub growth. Making measurements at higher elevations targets shrubs occupying the successional limit of species that will expand into new areas in the future. According to the generally accepted view, we expected that patches dominated by shrubs would have lower albedo values (e.g. Pearson *et al.*, 2013) throughout the growing season than the surrounding short-statured vegetation or bare ground. To put our results into a broader context, we calculated how the species-based albedo dynamics affect growing season energy budgets of tundra and we used the MCD43A3 MODIS albedo product to determine whether field measurements can be scaled to satellite measurements.

Materials and methods

Field albedo measurements

Albedo was measured during the 2012 and 2013 growing seasons at six locations along a 200 m north–south transect that paralleled the drainage axis in an alpine valley in the Ruby Ranges of south-west Yukon (61.2°N; 138.3°W). The vegetation along this transect was typical of plant cover at different stages of succession and shrub encroachment (Danby *et al.*, 2011). Furthermore, the shrub species included in our study were characteristic of shrub communities throughout the western Canadian Arctic (Myers-Smith, 2011). The six plots were at a similar elevation, descending slightly from south (1640 m) to north (1623 m). The sites along the transect represent the major vegetation types of the alpine tundra; no wet acidic tundra occurs at this location and no standing water was observed near the plots. The six sites are identified as *Salix pulchra* (Fig. 1, sites A-C), *Carex* (Fig. 1, site D), *Betula glandulosa* (Fig. 1, site E) and *Dryas*/Lichen dry tundra (Fig. 1, site F). The three *Salix pulchra* sites form a gradient in cover between 48% and 99% shrub cover. Plant community composition was assessed using the point intercept method (100 contacts every 0.05 m in a 0.50 m point quadrat), and each site was characterized by a single dominant species (Table 1). As *S. pulchra* is the dominant patch-forming shrub in the study area, a more detailed gradient of cover for this species was included in our study design. Only low-statured forms of *B. glandulosa* are found in the study area.

An albedometer (upward and downward facing CMP11 pyranometers, CMA11, Kipp & Zonen, Delft, the Netherlands)

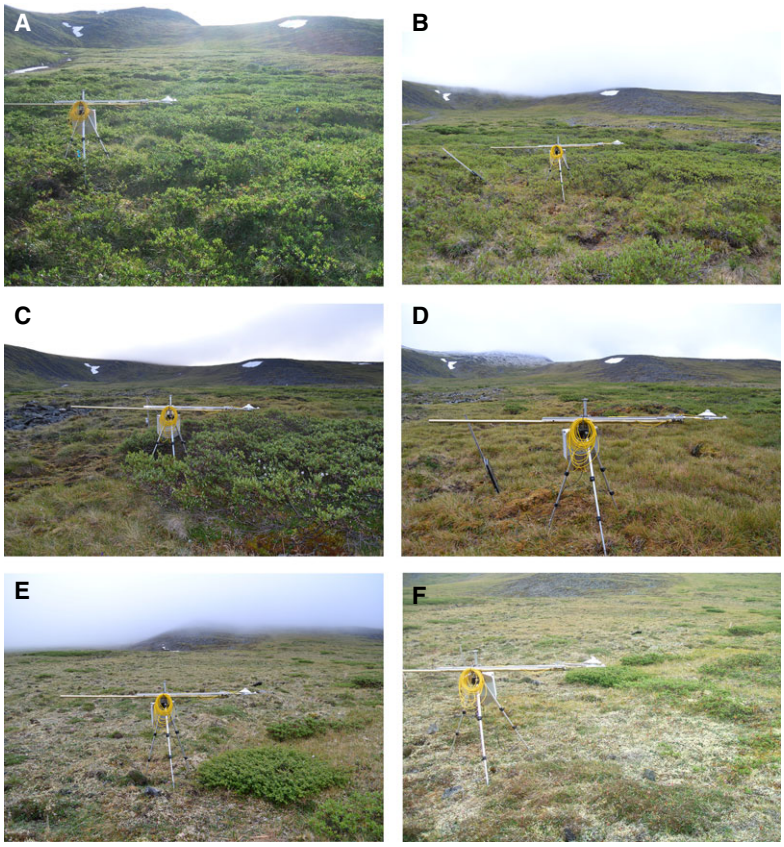

Fig. 1 Six tundra vegetation cover types considered in this study: *Salix pulchra* (site A- Sparse canopy; site B – Mid canopy; site C – Dense canopy), *Carex* (site D), *Betula glandulosa* (site E) and *Dryas/Lichen* dry tundra (site F). Detailed site characteristics are provided in Table 1.

was mounted at fixed positions over the patches of tundra being monitored. This albedometer is sensitive to short wave radiation between 285 and 2800 nm and is the highest precision class instrument manufactured by Kipp & Zonen. The maximum temperature response of the CMA11 is <1% for the growing-season temperature range found in the study area (−10–40 °C), and the maximum spectral selectivity is <3% between 350 and 1500 nm. The albedometer was positioned 1 m above each canopy type to minimize possible contamination from surrounding vegetation (Fig. 1) and was alternated among the six sites between 28 June 2012 and 15 August 2012. Sites were measured 5–6 times over the growing season at approximately weekly intervals, recording at least one diurnal cycle of 1-min averages. The observations used to compare albedo across sites were limited to 1 h before and after solar noon, when the sun was at its highest elevation and albedo was at, or close to, its daily minimum (Ohmura, 1981). If compromised by obstruction of the sensor (by snow, rain or fog), data were removed from the analysis; these conditions were identified using time series of incoming solar radiation from the upper channel of the albedometer, observations from a nearby meteorological station (Campbell Scientific, Edmonton, AB, Canada) and daily field observations of weather conditions. Talus patches are common throughout the valley (~20% of the surface), and albedo of a talus reference site was measured on 13 August 2012; a different talus reference site was measured on 15 July 2013.

Sites were resampled, under clear-sky conditions within 2 h of solar noon, on 15 July 2013 and 29 July 2013, using 1-min intervals for 10 min at each site. The 2013 sampling methodology was adjusted from that of 2012 to collect albedo values for all of the sites on the same day under direct sunlight. Analysis of the variance of 2012 albedo values indicated that under direct sunlight, 10 min was sufficient to collect a representative albedo measurement. Finally, four additional albedo measurements of *B. glandulosa* were made on 14 and 15 July 2013: three measurements were conducted 200 m north of the north end of the transect (lowest elevation – 1615 m) and one measurement was made at the south end (highest transect elevation – 1640 m). One moss site and an additional talus site, both in the middle of the transect, were measured on 15 July 2013.

Field spectral reflectance measurements

To further understand the shrub structural contributions to albedo and to provide an independent perspective on the albedometer measurements, we conducted spectral reflectance

Table 1 Site characteristics for representative tundra plant communities. Dominant plant cover is presented as a percentage of plot area and was assessed using the point intercept method. Vascular plants were identified to species, but are grouped here to the main functional types of interest. Cover by different plant groups overlaps, so percentages do not sum to 100%. Mean growing-season albedo (±SD) is the average of measurements acquired 1 h around solar noon during July and August for 2012. The 2013 albedo values (±SD) are the averages of 15 July and 29 July measurements recorded over 10 min at each site under direct sunlight within 2 h of solar noon. (**Carex* sp. predominantly *C. consimilis;* ** Dwarf *Salix* – *S. reticulata* and *S. polaris*)

Site	A	B	C	D	E	F
General description	Sparse *Salix*	Mid *Salix*	Dense *Salix*	*Carex*	*Betula*	*Dryas*/lichen
Betula glandulosa	0	0	0	0	100	0
Salix pulchra	48	88	99	0	0	0
Graminoid*	62	45	6	95	3	19
Moss	77	19	71	42	0	2
Dryas octopetala	0	0	0	0	0	52
Lichen	0	0	0	0	0	34
Dwarf *Salix***	0	33	0	36	0	16
Forbs	28	45	23	1	3	24
Canopy height (m)	0.20	0.51	0.55	0.15	0.17	0.01
2012 Mean Albedo	0.165 ± 0.003	0.144 ± 0.002	0.136 ± 0.002	0.183 ± 0.003	0.191 ± 0.002	0.190 ± 0.003
15 July 2013 Albedo	0.169 ± 0.001	0.144 ± 0.001	0.156 ± 0.002	0.193 ± 0.001	0.194 ± 0.001	0.191 ± 0.001
29 July 2013 Albedo	0.164 ± 0.001	0.155 ± 0.001	0.164 ± 0.002	0.199 ± 0.001	0.197 ± 0.002	0.208 ± 0.001
2013 Mean Albedo	0.167 ± 0.001	0.150 ± 0.001	0.160 ± 0.003	0.196 ± 0.001	0.196 ± 0.002	0.199 ± 0.001

measurements of the selected vegetation types. On 15 August 2012, the six transect sites were scanned five times each, over 1 min, with a full-range radiometrically calibrated spectroradiometer (PSR-3500, Spectral Evolution, Lawrence, MA, USA) using a 25° field of view foreoptic, 1 m above ground. These scans provide spectral reflectance measurements, measured as the hemispherical–conical reflectance factor (HCRF; Schaepman-Strub *et al.*, 2006) and allowed for analysis of fine-scale spectral features that provide information on the influence of canopy properties, such as leaf area index (LAI), on albedo. Because the PSR-3500 is a single-channel instrument that requires clear-sky conditions for high quality scans, spectra were only collected on this one occasion. To further normalize for variation in lighting conditions and calculate spectral reflectance, a scan of a 99% reflectance white standard (Spectralon, LabSphere, North Sutton, NH, USA) preceded each vegetation radiance measurement. The spectral range of the PSR-3500 is 350–2500 nm, with spectral resolution of 3.5 nm over the 350–1000 nm range; 10 at 1500; and 7 nm at 2100 nm. For comparison with albedometer readings, albedo was also calculated from spectral reflectance using a simple average of the reflectance values for all bandwidths between 350 and 2100 nm, disregarding the atmospheric absorption bands (350–399, 1361–1409, 1801–1959, 2401–2500 nm) that lacked sufficient energy to provide an adequate signal-to-noise ratio.

MODIS albedo

MODIS MCD43A3 albedo, generated from both the Terra and Aqua platforms, was used to determine the snow-covered albedo of the study site before and after the growing season when field albedo measurements were unavailable. These MODIS snow-covered albedo measurements of albedo appear in the energy balance calculation (next section below). MODIS growing-season albedo dynamics were also determined for our site for comparison with field measurements. Eight-day composites of MODIS MCD43A3 were downloaded from NASA's Earth Observing System Data and Information System at http://reverb.echo.nasa.gov, from 1 March 2000 to 13 August 2013; the white-sky and black-sky short wave (300–5000 nm) albedo products were used in this study. However, the majority of energy in solar radiation is found in the 300–2500 nm spectral range, which closely matched the range of our field spectrometer. White-sky albedo is the bihemispherical reflectance in isotropic illumination conditions, which therefore has the angular dependency eliminated. The MODIS black-sky albedo is the directional hemispherical reflectance, calculated in the MCD43A3 product for local solar noon. The MODIS albedo data were resampled from the native sinusoidal projection to Albers Conformal Conic using the nearest neighbour algorithm to 500 m grid cells in the NAD83 datum. White-sky and black-sky shortwave albedo values were extracted for the grid cell in which both the meteorological monitoring station and the summer albedo transect were situated. Due to cloud cover for most of the early growing season, few MODIS albedo values were available for direct comparison with the 2012 field data. Consequently, we aggregated the 2000 – 2013 MODIS short-wave albedo values, irrespective of quality flag, to obtain a full growing-season data set to determine whether a growing-season albedo increase could be observed. The MODIS albedo provided a better assessment of snow-covered albedo for our study site than could be obtained using literature values, even when using the 'poor quality flag' measurements. Also, it has been shown that the 'poor quality' MODIS albedo values produced using the magnitude inversion method for albedo generation with an *a priori* knowledge backup algorithm, performed well under most circumstances (Jin *et al.*, 2003a,b).

Solar radiation energy budget calculations

To further evaluate the relevance of seasonal albedo changes in a broader context, we calculated the change in surface energy balance at our site resulting from the influences of an increase in albedo over a longer snow-free growing season and the decrease in albedo from the change in the snow-covered period. These calculations were made using average albedo values of the dominant land cover types from field measurements and average albedo values for snow-covered periods extracted for the study site from the MODIS satellite sensor.

For this analysis, we calculated incoming solar radiation (W m^{-2}) for conditions (i) with no clouds and (ii) with 70% cloud cover (typical at our site), using the three models (solrad version 1.2) available from Washington State Department of Ecology (http://www.ecy.wa.gov/programs/eap/models.html). Values of incoming solar radiation were compared with instrumental measurements (CM6b pyranometer, Kipp & Zonen, Delft, the Netherlands) recorded at the meteorological station located at our study site for the period between 21 June 2012 and 30 December 2012. The scatter of the instrumental data was related to daily changes in cloud cover and consistent with our decision to use 70% cloud cover as a mean value for the entire season in these example calculations. Cloud cover was estimated as the ratio of measured solar radiation to 0% cloud covered modelled radiation. The daily average energy flux was then calculated as the average of the three global models (Ryan & Stolzenbach, 1972; Bras, 1990; Bird & Hulstrom, 1991) using a 70% cloud cover parameter and default settings, and converted to absorbed energy using the conversion 1 MJ m^{-2} day = 11.574 W m^{-2}. The total change in shortwave surface energy absorption (MJ m^{-2}) was calculated as the albedo change multiplied by the daily average solar flux (W m^{-2}), summed over the number of days over which the changes took place. The additional energy absorbed due to a reduction in snow cover was calculated as the difference between snow albedo derived from the average of MODIS MCD43A3 black-sky and white-sky albedos (0.58 – spring 2012 and 0.50 – fall 2012) and average field measured albedo of snow-free ground (0.14), multiplied by the daily average solar flux. This spring albedo difference was 0.44 and the fall albedo difference was 0.36, which were used to estimate the albedo change related to snow cover changes. These daily values were summed over the number of days of change in snow cover during the past decade (Zeng *et al.*, 2011; Brown *et al.* 2010). The reduction in snow cover for spring was estimated to be 11 days (2–12 June), and the delay in onset of permanent snow cover in the fall was 2 days (7–8 November).

The decrease in heating caused by the growing-season albedo increase for the area-averaged albedo for the study site using field measurements was calculated using a linear increase in albedo from 13 June to the maximum albedo at 28 July and then a subsequent linear albedo reduction to November 6. A high-resolution land cover map (Olthof & Fraser, 2007) resampled to the MODIS grid cell covering the study area indicated that deciduous shrub and graminoid cover were estimated at 20% each, with the remainder of the cover comprised of bare rock and soil. Using the high-resolution land cover map and field estimates of different land cover types, an area-average albedo increase of 0.02 for the growing season was calculated. The conversion of radiant flux to surface energy was calculated as outlined for snow cover change and was the cumulative sum of absorbed energy between 13 June and 6 November.

Statistical analyses

To assess overall differences in the seasonal patterns of average albedo, we used generalized additive mixed models (GAMM; Zuur *et al.*, 2009), including an interaction term between date (Day of Year) and site. Site was included as a random factor to account for the nested structure of the data. Differences in seasonal patterns among sites were evaluated by comparing models with and without the interaction term using a log-likelihood ratio test (LRT; Zuur *et al.*, 2009). All GAMM analyses were conducted in R 2.14.0 (R Development Core Team, 2011) with the *mgcv* (Wood, 2006) package.

Results

At the beginning of the 2012 measurement period, recently emerged shrub leaves, stems and branches were visible; green graminoids were just visible above the previous year's senesced material. By the end of the measurement period, deciduous leaves obscured more of the understory but showed no visible signs of senescence; *Carex* spp. displayed yellowing by 10 August 2012. Dry tundra appeared unchanged in composition and phenology through the duration of the experiment. Albedo patterns for the six land cover types were species-dependent, but most land covers showed increasing albedo during the 2012 summer growing season (Fig. 2a), and the timing of maximum and minimum albedo was different for each land cover type.

A significant interaction between 2012 Day of Year and Vegetation Type (LRT = 6554.96, $P < 0.001$) indicates different albedo trajectories for the six sites over the season. Sites with a dense deciduous shrub canopy component became more reflective as the growing season progressed (mid and dense canopy *Salix* (B & C) and dense canopy *B. glandulosa* (E)), whereas graminoid-dominated (D), sparse canopy *Salix* (A) and dry tundra (F) sites, which had either sparse or no shrub canopy, had relatively flat albedo trajectories. In 2012, shrub albedo values ranged from a high of 0.21 for mid-summer *B. glandulosa* to a low of 0.12 for early season *S. pulchra*. The 2013 albedo values (Table 1) followed the 2012 trend and were slightly higher, as expected for measurements made under direct sunlight (Ohmura, 1981).

The correlation of the PSR-3500 spectral reflectance measurements and the CMA-11 albedo values collected between August 8 and 13 2012 was $R^2 = 0.97$ using five

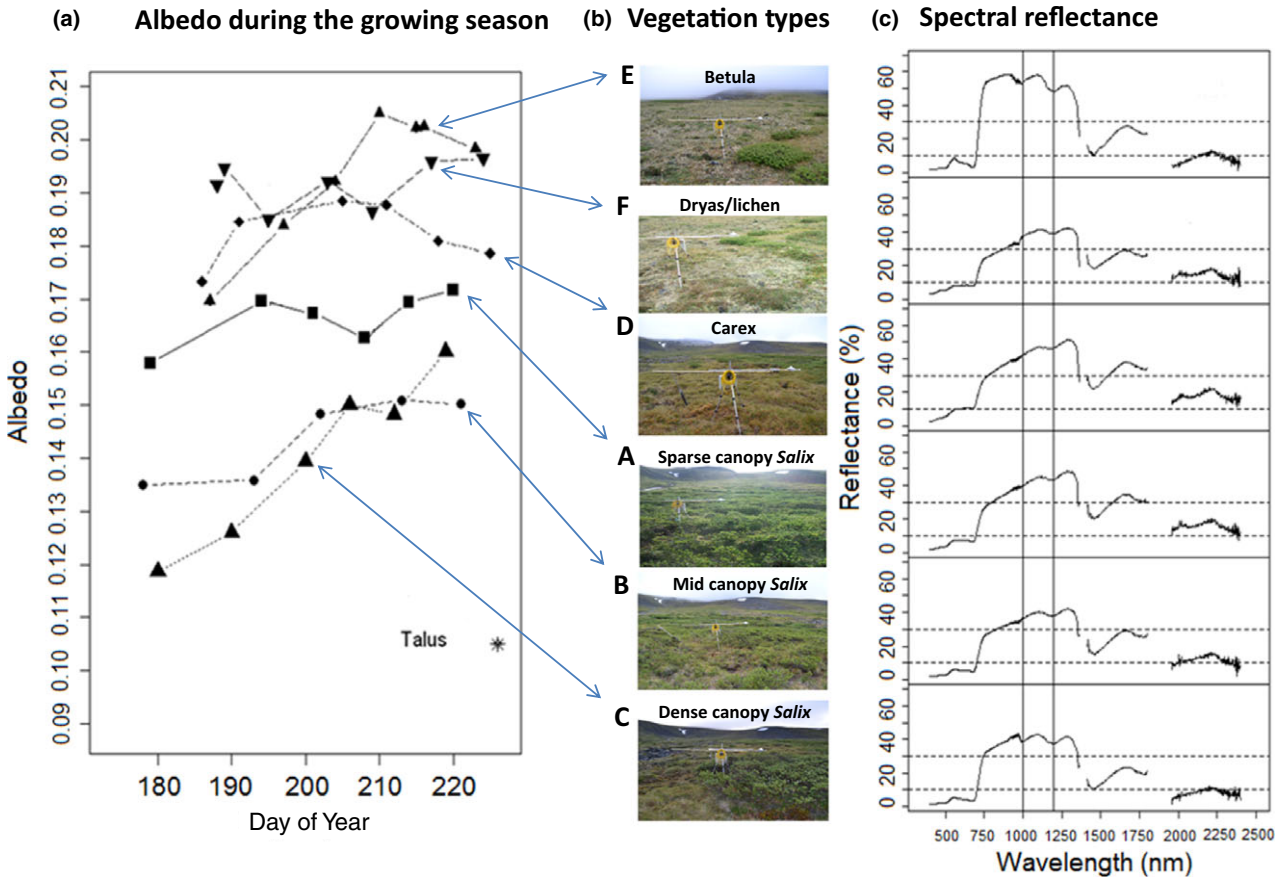

Fig. 2 Characteristics of the six dominant vegetation types. (a) Average broadband albedo during June, July and August 2012 calculated for 1 h before and after solar noon, compiled from 1-min averages for the six vegetation cover types; standard deviations for albedo measurements ranged from 0.001 to 0.006 indicating the standard errors are on the same order of size as the point symbols; thus, no error bars are included. (b) Photographs of the six sites. (c) Spectral reflectance of the 6 sites on 15 August 2012. Reflectance values for wavelengths affected by atmospheric water content have been removed. The depths of troughs at ~1000 and ~1200 nm (vertical lines) are indicative of leaf area index (LAI), where deeper troughs typically indicate higher LAI. The two dotted horizontal lines at reflectance values of 10% and 30% are for reference.

of the six sites. For this correlation, the dry tundra site was omitted because the spatial heterogeneity of *Dryas* and lichen ground cover resulted in different sampling footprints for the albedometer and the spectroradiometer. The high correlation between these independent measures of albedo indicated that the cosine field of view of CMA-11 provided a good representation of a discrete patch of tundra for the five sites when measured at 1 m above the ground.

Several additional albedo measurements of *B. glandulosa* shrubs near the transect were made on 14 and 15 July 2013, to place the albedo values measured for *B. glandulosa* on the transect into context. The average albedo for the three northern low elevation plots was 0.161 ± 0.013. The average canopy height was 0.20 ± 0.10 m. The additional *B. glandulosa* plot at the southern elevational limit had an albedo of 0.20 ± 0.01 and had a canopy height of 0.24 m. The additional sites were uniform in appearance and in the case of the shrubs were fully closed canopies. The albedo for moss that was collected in the middle of the transect was 0.126 ± 0.006. An additional talus patch was also measured to represent a typical value for a region devoid of vegetation and had an albedo of 0.087 ± 0.001. The additional sites were collected under direct sunlight near solar noon indicating the albedo values should be approaching the minimum diurnal values. The 2013 transect resampling confirmed the 2012 increase in growing-season albedo for canopy-forming landscape units. Further, the 2013 average albedo is larger than 2012 because only midsummer values were used in this calculation.

The average of the three models for incoming solar flux was 141.17 ± 80.39 W m^{-2} (one standard

deviation) for the period from 21 June to 8 November, 2012 (Fig. 3). This was the period for which field measurements of incoming solar radiation were available and albedo was less than maximum winter values. This model average value was close to the average incoming solar radiation measured at this station, 143.76 ± 89.51 W m^{-2}, over the same period, which supported our decision to use the 70% cloud cover scenario. For comparison, the average of the three models for the 0% cloud cover parameterization over the same period was 178.96 ± 102.53 W m^{-2}.

The effects of albedo dynamics on the overall surface energy balance (Fig. 4) indicate that a decrease in spring snow cover of 11 days will contribute an additional 103.9 MJ m^{-2} of surface heating, while the delay in snow cover of 2 days in the fall will contribute 0.95 MJ m^{-2}. In contrast, our field measurements indicate that an average increase in summer albedo of 0.02 (0.14 to 0.16) due to vegetation growth counteracts heating associated with the reduction in snow cover by 37.3 MJ m^{-2} (Fig. 4).

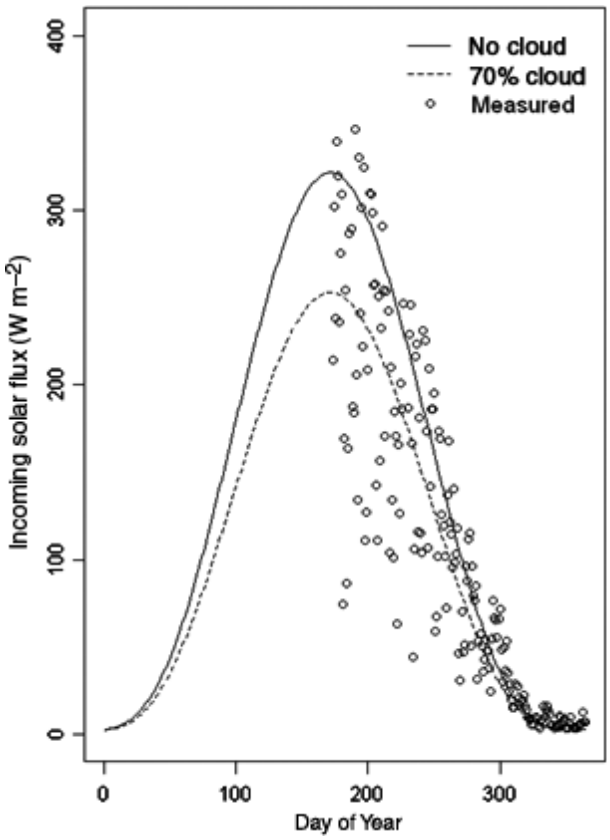

Fig. 3 Modelled daily average incoming solar radiation with no clouds (solid line) and with 70% cloud cover (dashed line) for the second half of 2012. Instrumental values (open circles) are shown for CM6b field measurements of daily average incoming solar radiation between 21 June 2012 and 30 December 2012.

The 2000 – 2013 aggregated MODIS black-sky and white-sky albedos displayed a growing season increase consistent with field measurements conducted within the same MODIS cell (Fig. 5). The black-sky albedo increased from a minimum of 0.138 to a maximum of 0.147, while the white-sky albedo increased from a minimum of 0.146 to a maximum of 0.160. Intermittent snow cover in several years caused the late summer albedo increase and subsequent large standard error on Day of Year 241.

Discussion

Our albedo field measurements show an increase in tundra summer albedo, with a dominant shrub,

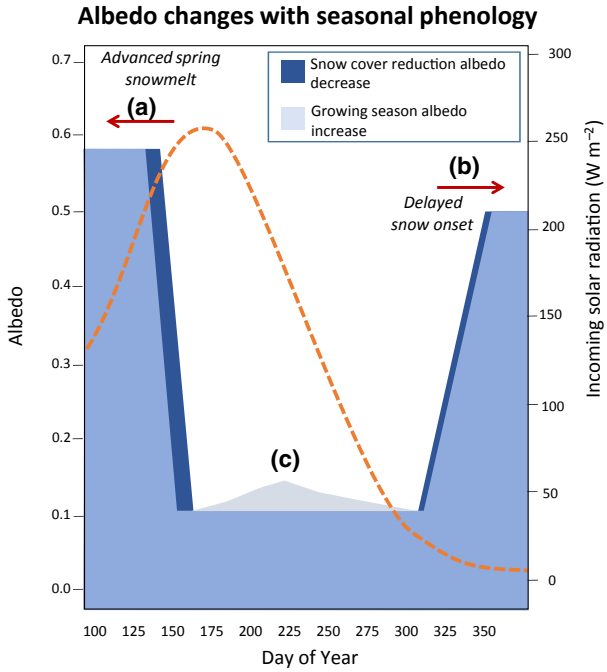

Fig. 4 Conceptual model of albedo change related to seasonal phenology. The potential for increasing growing-season albedo in tundra landscapes has been attributed to advanced spring snow melt (a) and delayed onset of snow at the end of summer (b). The darker areas represent the amount of increased heating attributed to a change in snow cover albedo. This influence will generally be much greater in spring compared to late summer because there is more incoming solar radiation earlier in the season (dashed line; W/m2, data calculated at 61.2°N; 138.3°W for 70% cloud cover which was the decadal average cloud over from 2000 to 2010 at our study site). Based on our measurements in Fig. 2, summer (2012) average albedo will be greatest near the end of the growing season (c corresponds to mid August; grey–blue); however, the average increase in albedo over the snow-free season has the potential to partially negate increased heating caused by advanced snow melt or delayed onset when calculated for the entire snow-free season.

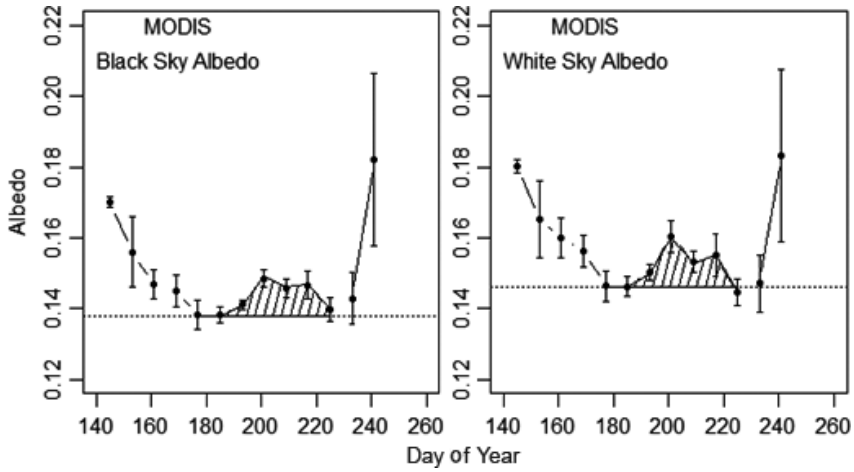

Fig. 5 MODIS MCD43A3 short-wave black-sky and white-sky albedo values aggregated for the 2000 to 2013 growing season (day of year 145 to 241) in the 500 m grid cell covering the field measurement transect. Error bars are standard errors. Dashed horizontal lines indicate minimum MODIS black-sky and white-sky albedo values. The shaded increase represents the cumulative increase in growing-season albedo. Intermittent snow cover at this alpine location is the cause of the large increase in albedo at Day of Year 241 at the end of the growing season.

B. glandulosa, reaching the highest values at peak growing season. These results challenge the generally accepted view of shrub-covered areas having low albedo in tundra land cover, particularly when compared to the background albedo (e.g. talus) for this site. Furthermore, future efforts to calculate energy budgets and a sensible heating feedback in the Arctic will require more detailed information about the relative abundance of different ground cover types, particularly shrub species and their respective growth forms and phenology. Our detailed field measurements repeated at the exact same sites allow fine-scale characterization of phenological changes in albedo at sites that are broadly representative of tundra vegetation at different stages of succession and shrub encroachment (Danby *et al.*, 2011). Further, the shrub species investigated here are characteristic of much of the western Arctic (Myers-Smith, 2011), and belong to the main genera of tundra shrubs (Walker *et al.*, 2005).

Albedo values of *Salix* stands were lower than shrub-free vegetated sites and albedo decreased as shrub cover increased (sparse to dense *Salix* canopy at sites A-C, Fig. 2; Table 1). These results are consistent with theory (Oke, 1987) and previous studies (e.g. Thompson *et al.*, 2004). However, mean albedo was highest for the closed-canopy *B. glandulosa* and dry tundra (sites E & F); and these plots had summer-averaged albedo values similar to vegetated sites lacking shrubs (*Carex*- and *Dryas*/lichen-covered sites). The albedo values reported here for short-statured *B. glandulosa* are bracketed by both higher (Blok *et al.*, 2011) and lower (Beringer *et al.*, 2005) values reported for other Arctic sites, but it is difficult to determine the cause of this variation because the physical determination of albedo and the spatial sampling regimes employed by all of these studies are different.

For all shrub sites observed here, minimum albedo occurred early in the growing season, immediately following snow melt (Fig. 2a), and then continued to increase over much of the summer. Growing-season albedo values are usually measured at or around point C in Fig. 4, which indicates that the albedo for snow-off period is overestimated if this is the only measure of albedo used for the whole season. Our early season measurements of *B. glandulosa* and *S. pulchra* are similar to the end of snow melt albedo for two similar vegetation classes measured in Alaska (Sturm *et al.*, 2005): tundra dominated by 20 cm high *B. nana*, and tall shrub dominated by 110 cm high *S. pulchra* and *B. glandulosa*. Furthermore, the short-statured deciduous shrubs with dense canopy cover examined here exhibited increasing albedo throughout the growing season, consistent with observations made by Blanken & Rouse (1994) for a willow and birch stand near Churchill, Manitoba. Moreover, tundra vegetation plots that had dense shrub canopies displayed the maximum increase in albedo of all plots monitored throughout the growing season in our study. Weller & Holmgren (1974) also found a similar increase in albedo as short-statured (<12 cm in height) dry tundra on flat terrain at Barrow transitioned from spring melt to growing season, but this response was modulated by the amount of standing water.

The *S. pulchra* plot with the smallest canopy cover (48%) and the largest moss cover (77%; site A) had the

highest albedo value for the three *Salix* plots. Although moss has lower albedo values than the vegetated sites studied (indicated by the measurement of the moss site), a high coverage of graminoids at site A (Table 1) creates a highly reflective canopy, mitigating the effect that moss has on lowering the plot's albedo. The vegetation albedo values are much larger than the reference albedo of bare talus, which ranged between 0.087 and 0.102 (our study), and 0.11 for Barren Tundra as measured by Blok *et al.* (2011), indicating that, relative to bare mineral surface, shrub expansion can actually *increase* albedo.

Daily cloud cover for the growing season of 2012 did not show a significant change (increase or decrease) over the study period, which indicates that cloud cover increase, and the resulting increase in diffuse solar radiation, was not responsible for the increasing growing season trend in albedo. Instead, the mechanism of this seasonal increase in albedo was revealed by examining 2012 reflectance spectra; as leaves expand and the shrub canopy surface becomes increasingly impenetrable by solar radiation towards midsummer, the increase in optical scattering in the near-infrared (NIR) portion of the electromagnetic spectrum increases the overall albedo (Fig. 2). This increase in NIR reflectance (Fig. 2c), particularly in the shrub plots, illustrates the effect of canopy structure on albedo caused by increased leaf area index (Lafleur *et al.*, 1987; Asner, 1998). Troughs at ~1000 and ~1200 nm are indicative of water absorption, with deeper troughs indicating higher LAI (Zheng & Moskal, 2009), as a result of greater amount of water stored within the canopy leaves of larger canopies (Sims & Gamon, 2003). In general, we observed an increase in LAI and NIR reflectance as shrub canopy cover increased. LAI estimated from reflectance spectra of *B. glandulosa* appears higher than for *S. pulchra*. We have used the relationship between LAI and water band absorption to describe the general patterns, but further work will be required to derive precise relationships between the different canopy properties and albedo for the shrub species investigated here.

Although the rate of succession from tundra to shrub and the associated changes in albedo will occur over decades, any replacement of bare ground (Elmendorf *et al.*, 2012) or talus with vegetation will increase growing-season albedo. The establishment of vegetation within talus patches, which exhibited the lowest albedo of any cover type reported here, is a slow successional process (Danby *et al.*, 2011), and will likely occur over a longer period than shrub encroachment or infilling. To put these seasonal increases in albedo into context, in our study, dense canopy shrub cover increased their albedo by approximately 40% during the summer, which is as large as the range of albedo values from forest to tundra (Thompson *et al.*, 2004). The albedo differences between tundra vegetation classes are relatively small (peak growing-season albedo difference between tundra classes (Barren, Graminoid and Shrub) is approximately 3–4%), and entire summer differences in energy balance have been measured to be 3–5% greater for forest than tundra (Lafleur *et al.*, 1992). This suggests that changes between tundra vegetation classes will produce modest changes in energy balance over the next century, even if successional changes are relatively rapid. Forecasting future albedo and surface energy balance for tundra communities must consider the rate of vegetation change, shrub encroachment, grazing, snow accumulation and other processes (Cohen *et al.*, 2013). Short-statured shrubs (<0.5 m) are expected to increase in abundance in many regions (Bret-Harte *et al.*, 2001; Epstein *et al.*, 2004), cover (Pearson *et al.*, 2013) and height (Walker *et al.*, 2006), and recent studies indicate that *Betula* spp. in particular are likely to thrive in a warmer Arctic (Euskirchen *et al.*, 2009; Heskel *et al.*, 2013). These predictions, along with the results presented here, suggest that summertime albedo may actually increase with Arctic shrub encroachment and diminish surface warming as a result.

Spatial patterns associated with shrub cover change include species-specific infilling, individual expansion (Tape *et al.*, 2006) and establishment of new stems in bare ground (Tape *et al.*, 2012; Frost & Epstein, 2014). All of these processes must be considered when making projections of future shrub-dominated tundra albedo and energy balance. If the projection of low-statured shrub cover increase is accurate and it outpaces the increases in tall statured growth (i.e. *Betula* spp. gains more than *Salix* spp.), then future landscape level tundra albedo taken as a whole might not necessarily decrease (Blok *et al.*, 2011), as currently hypothesized (Chapin *et al.*, 2005; Pearson *et al.*, 2013). However, Blok *et al.* (2011) collected albedo values between July 12 and August 13 and missed the actual minimum albedo values associated with preleaf shrub cover.

One consequence of these changes to shrub tundra is that albedo in the Arctic will be dependent on the relative expansion of different shrub species with contrasting growth forms, especially at decadal scales where shrubs are expected to respond to climate forcing more quickly than trees (Sturm *et al.*, 2001). Furthermore, the period of peak greenness in Arctic deciduous shrubs appears to be increasing (Sweet *et al.*, 2015), so it follows that the peak period of growing-season albedo for shrubs will also lengthen and increase the average summer growing-season albedo. In contrast, any increase in shrub cover and the associated growing season increase

in albedo can be countered by the decrease in winter albedo caused by branches in or above the snow (Sturm *et al.*, 2005), or changes related to surface moisture. Growing-season albedo can increase for sparsely vegetated tundra as it dries through the growing season (Harding & Lloyd, 1998) and more generally as tundra dries due to snow cover decrease, permafrost thaw and temperature increase in the Arctic. These changes will partially mitigate any effect of earlier snow melt on annual energy balance and act as a negative sensible heating feedback to climate on a decadal scale.

In this study, we provide empirical insights that showcase why many of the metrics used in land surface models (LSMs) are more complex and dynamic than often assumed. A coordinated approach to the validation of land surface model parameterizations should be designed and conducted and will require a community effort to benefit future prediction accuracy in climate models. However, even though our study site had only a modest (~20%) deciduous shrub cover, albedo increase related to growing season green-up for shrub-covered areas is detectable with MODIS. Based on the results presented here, we recommend that future LSMs and related energy balance calculations and feedback estimates for tundra land cover be informed by direct satellite measurements, supplemented by ground validation, rather than by assumed, fixed albedo measurements for individual land cover classes.

In conclusion, our study shows that the albedo of tundra vegetation increases from snow melt to the peak of the growing season differently for different vegetation types. Shrub species showed a large difference in albedo values, where *Betula* had the highest albedo and *Salix* the lowest, and increases in albedo were largest for shrubs with closed canopies. This increase in summer albedo acts to partially negate the effect of earlier spring snow melt on surface energy balance. More detailed landscape albedo characterizations, especially those derived from remote sensing and applied to ecosystem modelling, are required to develop more realistic growing-season albedo dynamics over tundra. These characterizations must include the relative abundance of different ground cover types, including barren and shrub species adjusted for growth forms and phenology, and should also consider patterns of changing surface hydrology. The feedback relationships between energy budgets and land cover in the Arctic will require these more detailed observations and measurements, particularly for the beginning of the snow-free period and peak growing season. The sum of future albedo-mediated sensible heating feedbacks related to changes in tundra vegetation could be positive or negative, but will likely remain small in magnitude over at least the next several decades.

Acknowledgements

This research was supported by the Canada Foundation for Innovation, the Canada Research Chairs Program, the Natural Sciences and Engineering Research Council (Canada), Alberta Innovates Centre for Research Excellence, the W. Garfield Weston Foundation, Wildlife Conservation Society of Canada, the Consejeria de Educacion (JCCM, Spain) and the European Social Fund. The authors declare no conflict of interest.

References

Asner P (1998) Biophysical and biochemical sources of variability in canopy reflectance. *Remote Sensing of Environment*, **64**, 234–253.

Beringer J, Chapin FS, Thompson CC, McGuire AD (2005) Surface energy exchanges along a tundra-forest transition and feedbacks to climate. *Agricultural and Forest Meteorology*, **131**, 143–161.

Bird RE, Hulstrom RL (1991) *A Simplified Clear Sky model for Direct and Diffuse Insolation on Horizontal Surfaces*, pp. 1–46. SERI Technical Report SERI/TR-642-761. Solar Energy Research Institute, Golden, CO.

Blanken PD, Rouse WR (1994) The role of willow-birch forest in the surface energy balance at Arctic treeline. *Arctic and Alpine Research*, **26**, 403–411.

Blok D, Schaepman-Strub G, Bartholomeus H *et al.* (2011) The response of Arctic vegetation to the summer climate: relation between shrub cover, NDVI, surface albedo and temperature. *Environmental Research Letters*, **6**, 035502.

Bras RL (1990) *Hydrology*. Addison-Wesley, Reading, MA.

Bret-Harte MS, Shaver GR, Zoerner JP *et al.* (2001) Developmental plasticity allows *Betula nana* to dominate tundra subjected to an altered environment. *Ecology*, **82**, 18–32.

Brown R, Derksen C, Wang L (2010) A multi-data set analysis of variability and change in Arctic spring snow cover extent, 1967–2008. *Journal of Geophysical Research*, **115**, D16111, doi:10.1029/2010JD013975.

Chapin FS, Strum M, Serreze MC *et al.* (2005) Role of land-surface changes in Arctic summer warming. *Science*, **310**, 657–660.

Cohen J, Pulliainen J, Ménard CB *et al.* (2013) Effects of reindeer grazing on snowmelt, albedo and energy balance based on satellite data analyses. *Remote Sensing of Environment*, **135**, 107–117.

Cook BI, Smerdon JE, Seager R, Coats S (2014) Global warming and 21st century drying. *Climate Dynamics*, **43**, 2607–2627.

Danby RK, Koh S, Hik DS, Price LW (2011) Four decades of plant community change in the alpine tundra of southwest Yukon, Canada. *Ambio*, **40**, 660–671.

Elmendorf SC, Henry GHR, Hollister RD *et al.* (2012) Plot-scale evidence of tundra change and links to recent summer warming. *Nature Climate Change*, **2**, 453–457.

Epstein HE, Calef MP, Walker MD, Chapin FS, Starfield AM (2004) Detecting changes in arctic tundra plant communities in response to warming over decadal time scales. *Global Change Biology*, **10**, 1325–1334.

Eugster W, Rouse WR, Pielke RA *et al.* (2000) Land-atmosphere energy exchange in Arctic tundra and boreal forest: available data and feedbacks to climate. *Global Change Biology*, **6**, 84–115.

Euskirchen ES, McGuire AD, Chapin FS, Thompson CC (2009) Changes in vegetation in northern Alaska under scenarios of climate change, 2003-2100: implications for climate feedbacks. *Ecological Applications*, **19**, 1022–1043.

Frost GV, Epstein HE (2014) Tall shrub expansion in Siberian tundra ecotones since the 1960s. *Global Change Biology*, **20**, 1264–1277.

Hallinger M, Manthey M, Wilmking M (2010) Establishing a missing link: warm summers and winter snow cover promote shrub expansion into alpine tundra in Scandinavia. *New Phytologist*, **186**, 890–899.

Harding RJ, Lloyd CR (1998) Fluxes of water and energy from three high latitude tundra sites in Svalbard. *Nordic Hydrology*, **29**, 267–284.

Heskel M, Greaves H, Kornfeld A *et al.* (2013) Differential physiological responses to environmental change promote woody shrub expansion. *Ecology and Evolution*, **3**, 1149–1162.

Jin Y, Schaaf CB, Woodcock CE *et al.* (2003a) Consistency of MODIS surface BRDF/Albedo retrievals: 1. Algorithm performance. *Journal of Geophysical Research*, **108**, D54158.

Jin Y, Schaaf CB, Woodcock CE *et al.* (2003b) Consistency of MODIS surface BRDF/Albedo retrievals: 2. Validation. *Journal of Geophysical Research*, **108**, D54159.

Lafleur PM, Rouse WR, Hardill SG (1987) Components of the surface radiation balance of subarctic wetlands terrain units during the snow-free season. *Arctic and Alpine Research*, **19**, 53–63.

Lafleur PM, Rouse WR, Carlson DW (1992) Energy balance difference and the hydrologic impacts across the northern treeline. *International Journal of Climatology*, **12**, 193–203.

Moore KE, Fitzjarrald DR, Sakai RK (1996) Seasonal variation in radiative and turbulent exchange at a deciduous forest in central Massachusetts. *Journal of Applied Meteorology*, **35**, 122–134.

Myers-Smith IH (2011) Shrub encroachment in arctic and alpine tundra: Patterns of expansion and ecosystem impacts. PhD Thesis. University of Alberta, Edmonton, Canada.

Ohmura A (1981) *Climate and Energy Balance of Arctic Tundra*. Zürcher Geographische Schriften/ETH Zürich, Switzerland.

Oke TR (1987) *Boundary Layer Climates*, 2nd edn. Methuen, London.

Olthof I, Fraser RH (2007) Mapping northern land cover fractions using Landsat ETM+. *Remote Sensing of Environment*, **107**, 496–509.

Pearson RG, Phillips SJ, Loranty MM *et al*. (2013) Shifts in Arctic vegetation and associated feedbacks under climate change. *Nature Climate Change*, **3**, 673–677.

R Development Core Team (2011) *R: A Language and Environment for Statistical Computing*. R Foundation for Statistical Computing, Vienna, Austria. ISBN 3-900051-07-0; URL http://www.R-project.org/

Ryan PJ, Stolzenbach KD (1972) *Engineering Aspects of Heat Disposal From Power Generation* (ed. Harleman DRF). R.M. Parson Laboratory for Water Resources and Hydrodynamics, Department of Civil Engineering, Massachusetts Institute of Technology, Cambridge, MA.

Schaepman-Strub G, Schaepman ME, Painter TH, Dangel S, Martonchik JV (2006) Reflectance quantities in optical remote sensing – definitions and case studies. *Remote Sensing of Environment*, **103**, 27–42.

Sims DA, Gamon JA (2003) Estimation of vegetation water content and photosynthetic tissue area from spectral reflectance: a comparison of indices based on liquid water and chlorophyll absorption features. *Remote Sensing of Environment*, **84**, 526–537.

Snow, Water, Ice, Permafrost in the Arctic (SWIPA) (2011) Available at: http://amap.no/swipa (accessed 22 April 2013).

Sturm M, Racine C, Tape K (2001) Increasing shrub abundance in the Arctic. *Nature*, **411**, 546–547.

Sturm M, Douglas T, Racine C, Liston GE (2005) Changing snow and shrub conditions affect albedo with global implications. *Journal of Geophysical Research*, **110**, G01004.

Sweet SK, Griffin KL, Steltzer H, Gough L, Boelman NT (2015) Greater deciduous shrub abundance extends tundra peak season and increases modeled net CO_2 uptake. *Global Change Biology*, **21**, 2394–2409.

Tape K, Sturm M, Racine C (2006) The evidence for shrub expansion in Northern Alaska and the Pan-Arctic. *Global Change Biology*, **12**, 686–702.

Tape KD, Hallinger M, Welker JM, Ruess RW (2012) Landscape heterogeneity of shrub expansion in Arctic Alaska. *Ecosystems*, **15**, 711–724.

Thompson C, Beringer J, Chapin FS, McGuire AD (2004) Structural complexity and land-surface energy exchange along a gradient from arctic tundra to boreal forest. *Journal of Vegetation Science*, **15**, 397–406.

Walker DA, Raynolds MK, Daniëls FJ *et al*. (2005) The circumpolar Arctic vegetation map. *Journal of Vegetation Science*, **16**, 267–282.

Walker MD, Wahren H, Hollister RD *et al*. (2006) Plant community responses to experimental warming across the tundra biome. *Proceedings of the National Academy of Sciences of the United States of America*, **103**, 1342–1346.

Weller G, Holmgren G (1974) The microclimate of the Arctic tundra. *Journal of Applied Meteorology*, **13**, 854–862.

Wood SN (2006) *Generalized Additive Models: An Introduction With R*. Chapman and Hall/CRC, Boca Raton, Florida.

Zeng H, Jia G, Epstein H (2011) Recent changes in phenology over the northern high latitudes detected from multi-satellite data. *Environmental Research Letters*, **6**, 045508.

Zheng G, Moskal LM (2009) Retrieving Leaf Area Index (LAI) using remote sensing: theories, methods and sensors. *Sensors*, **9**, 2719–2745.

Zuur AF, Leno EN, Walker NJ, Saveliev AA, Smith GM (2009) *Mixed Effects Models and Extensions in Ecology with R*. Springer, New York.